Sustainable Energy & Fuels

COMMUNICATION

View Article Online
View Journal

Cite this: DOI: 10.1039/c8se00250a

Received 30th May 2018
Accepted 3rd July 2018

DOI: 10.1039/c8se00250a

rsc.li/sustainable-energy

Encapsulating perovskite solar cells to withstand damp heat and thermal cycling†

Rongrong Cheacharoen, [a] Caleb C. Boyd, [a] George F. Burkhard, [a] Tomas Leijtens, [a] James A. Raiford, [b] Kevin A. Bush, [a] Stacey F. Bent [b] and Michael D. McGehee *[ac]

Perovskite solar cells (PSCs) are highly promising, but they are mechanically fragile, composed of layers with mismatches in thermal expansion coefficients, and known to decompose in the presence of heat and moisture. Here we show the development of a glass–glass encapsulation methodology for PSCs that enables them to pass the industry standard IEC 61646 damp heat and thermal cycling tests. It is important to select a thermally stable perovskite composition to withstand the encapsulation process at 150 °C and design a cell that minimizes metal diffusion. Moreover, the package needs an edge seal to effectively prevent moisture ingress and an inert encapsulant with an appropriate elastic modulus to hold the package together while allowing for compliance during temperature fluctuations. Our work demonstrates that industrially relevant encapsulation techniques have the potential to enable the commercial viability of PSCs.

1 Introduction

Perovskite solar cells (PSC) are rapidly emerging, with power conversion efficiencies (PCE) above 22% [1] for a single junction and 23.6% in monolithic tandems with silicon.[2] However, various environmental and mechanical instabilities inhibit commercialization of PSCs. Heat or moisture can catalyze the evolution of volatile organic species and leave behind lead iodide.[3–6] Replacing methylammonium with less volatile cations and using a barrier can enhance thermal and moisture stability.[3,7,8] In addition, PSCs have low fracture energy[9] and multiple layers with mismatched coefficients of thermal expansion (CTE),[10] making them vulnerable to delamination. We recently demonstrated that PSCs packaged in compliant encapsulant survived temperature cycling between −40 °C and 85 °C.[10]

Encapsulation for PSCs needs to provide resilience against temperature and humidity extremes at a low cost for PSCs to be competitive with other commercial technologies. Some notable previous efforts utilized single-layer hydrophobic thin films[8,11] or multi-layer thin film encapsulation from other organic electronic technologies.[12] While the best result of thin film encapsulation has demonstrated a one year lifetime,[13] these films are easily punctured and the ones with high barrier qualities are still cost-prohibitive for commercialization. Another encapsulation method uses a UV-cured epoxy edge seal due to ease of processing at room temperature;[14,15] however, most epoxies are rigid and crack easily with temperature cycling.[16] A more holistic approach must be taken when designing PSC packaging: it must resist ingress of moisture at elevated temperatures, withstand temperature cycling without delamination, and enable efficient and stable operation.

Glass–glass encapsulation has enabled silicon solar cells to retain 95% PCE after 20 years in the field[17] and is a promising route for PSCs. Two critical components of a glass–glass package are the edge seal and encapsulant. The main function of an edge seal is to delay moisture ingress. An encapsulant, which fills in excess volume in the package, holds the package tightly together and ensures that the edge seal remains compressed throughout prolonged field exposure. It needs to have high transmission, high volume resistivity, no reactive chemical species, low moisture absorption, and high resistance to UV.[18] Glass–glass encapsulated PSCs with butyl rubber as both the edge seal and encapsulant performed well in a 540 hour damp-heat test.[19] Previously we demonstrated that glass–glass encapsulated PSCs with a butyl rubber edge seal and an ethylene vinyl acetate (EVA) encapsulant passed the 1000 hour damp-heat test.[2] While this latter result was encouraging, the packaged devices suffered from visible degradation that was accompanied by a noticeable drop in photocurrent, implying that the package could eventually fail.

In this work, we describe flaws identified in the design of a 1st generation glass–glass package and show substantial improvements for a 2nd generation package. We have used the

[a]Materials Science and Engineering, Stanford University, Stanford, CA, 94305, USA
[b]Chemical Engineering, Stanford University, Stanford, CA, 94305, USA
[c]Chemical and Biological Engineering, University of Colorado, Boulder, CO 80309, USA. E-mail: michael.mcgehee@colorado.edu

† Electronic supplementary information (ESI) available. See DOI: 10.1039/c8se00250a

International Electrotechnical Commission (IEC) 61646 standard for thin film modules[20] to accelerate different degradation pathways that would inhibit a 25 year lifetime of PSCs for commercialization. The pertinent tests for PSCs are the 1000 hour damp-heat test (85 °C-85% relative humidity (RH)) to assess their resilience to heat and moisture and the 200 thermal cycling test (between −40 °C and 85 °C) to probe delamination that stems from CTE mismatches. Our findings highlight the key design requirements for developing stable, packaged PSCs for long-term stability.

2 Encapsulation package design

It is critical to use thermally stable solar cell active layers for the 150 °C encapsulation process required for glass–glass packing. Therefore, we used a mixed cesium and formamidinium (FA) cation perovskite with a composition of $Cs_{0.17}FA_{0.83}Pb(Br_{0.17}I_{0.83})_3$ in this study for its high thermal stability.[21,22] We also utilized indium tin oxide (ITO) as a transparent electrode and a two-fold barrier: preventing organics or iodine species from escaping the perovskite and reacting with the top metal electrode,[23,24] and protecting the perovskite from trace moisture inside the package. PSCs in this study have the same layers (Fig. 1a) as the top cell of the 23.6% PCE perovskite-silicon monolithic tandem, so the findings presented here should translate well to the stability of the current world record Si-perovskite monolithic tandem device architecture.[2] We use a butyl rubber edge seal with added desiccant and a glass transition temperature below −50 °C because it can be compliant throughout temperature cycling;[25] it is also superb in delaying moisture ingress with two orders of magnitude lower Water Vapor Transmission Rate (WVTR) compared with UV-curable epoxies and polymeric encapsulants.[16,19] Lamination consists of a vacuuming and a pressing step. Since most encapsulants' melting points are below 100 °C,[26] they can flow during processing until they are fully cured. Once set, the encapsulant bonds the top glass to the bottom glass and maintains pressure on the rubber edge seal, preventing moisture ingress. It is important to ensure the volume of encapsulant matches the volume that needs to be filled; too much encapsulant pushes the edge seal out of place, while too little results in voids, which can either pull air in or cause the package to break.

Fig. 1b, d and e show side, top view, and an image of the 1st generation package. This design used evaporated metal fingers and soldered metal ribbons to conduct current from the cell to the outside. Both sides of the ribbon were covered with edge seal in order to minimize moisture ingress. Furthermore, the 2 cm × 2 cm solar cells substrates were packaged between two large pieces of glass and sheets of EVA encapsulant. Even though the 1st generation package enabled two PSCs to pass the IEC 61646 1000 hour damp heat test,[2] Fig. S1† reveals visible degradation both under the area protected by the top ITO, indicated by a green rectangle in Fig. 1d, and the area outside the protective ITO. After 1000 hours of damp heat, there was noticeable yellowing of the perovskite adjacent to the solder ribbon and the metal fingers on top of the ITO, which is indicative of metal-induced degradation of the perovskite causing yellow PbI_2 to form.[23,24] In the 2nd generation package, we used the transparent ITO electrode to separate perovskite from metal and made sure that there was 2 mm of lateral space between the evaporated metal and the PSCs (Fig. 1c and d). A thorough characterization of the metal-induced degradation will be presented in a separate manuscript.

In the 1st generation package, the entire area underneath the protective ITO showed signs of PbI_2 formation, indicating that the degradation is not only from reaction with the metal but also from moisture; we hypothesized that the moisture entered around the edges of the solar ribbon or was trapped in cavities created by PSC movement while the encapsulant was still in the

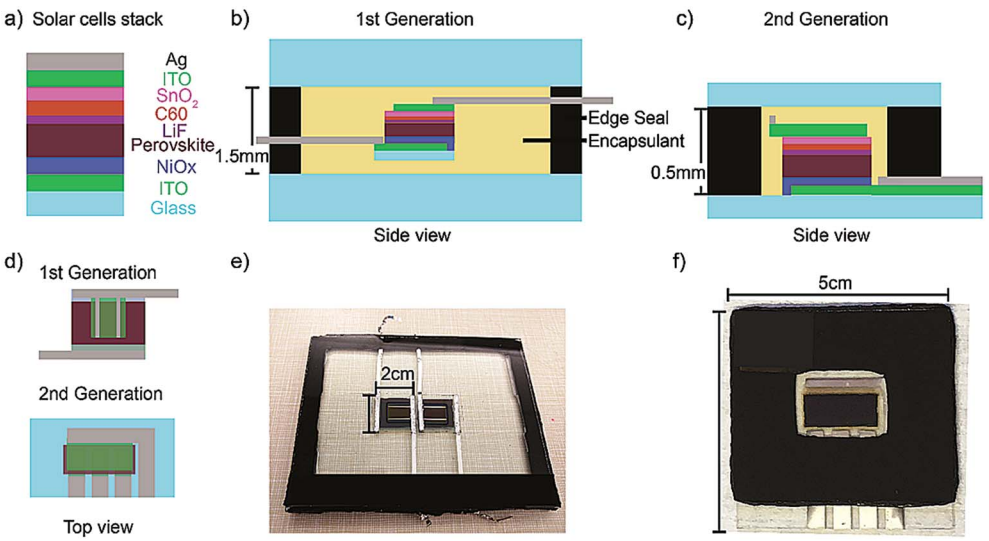

Fig. 1 (a) PSC stack in this study. Side view of (b) 1st generation (c) 2nd generation package assembly (not to scale). (d) Top view of both package generations. Top view image of (e) 1st generation (f) 2nd generation package after lamination.

molten state during lamination (Fig. S2a†). In the 2nd generation package, we fabricated PSCs and deposited electrical feedthroughs directly on one side of the glass cover to minimize moisture ingress and eliminate cavities formed by cell movement. Kempe *et al.* modeled a bond width of 1.25 cm for butyl rubber with added desiccant to be adequate for 25 year lifetime.[25] Therefore, we increased the butyl rubber edge seal bond width from 1 cm (1st generation) to 1.5 cm (2nd generation) to enhance its effectiveness in delaying moisture (Fig. 1e and f).

3 Encapsulant selection

We compare three types of commercial encapsulants including EVA, Surlyn, and polyolefins for thermal profile, elastic modulus, and chemical reactivity (Table 1). The exact chemical composition of the primary polymer or additives of these commercial encapsulants are not revealed by the providers. However, we prefer using these materials over simpler ones with known composition because they are highly optimized for commercial solar cell technologies. To rapidly screen for a suitable encapsulant for PSCs, we aged the 1st generation packages in an accelerated condition at 120 °C-100% RH for 20 hours and observed degradation features under a lamp, which is more illustrative than a room light (Fig. S3†). In the EVA package (Fig. 2a), yellow lines outside of the ITO show signs of the perovskite degrading into PbI_2, which is likely due to heat and moisture induced decomposition of the EVA into acetic acid,[27] which in turn reacted with the perovskite, as also confirmed in Fig. S3.† We also observed these yellow lines for EVA packaged PSCs after 1000 hours at 85 °C-85% RH, Fig. S1.† Since EVA likely reacts chemically with perovskites in damp heat conditions and has been implicated in potential induced degradation (PID) in Si solar panels,[28] it is not favorable for PSCs. In Surlyn encapsulated PSCs, the translucent area under the top ITO illustrates degradation of perovskite in contrast to the uncovered brown area outside where the perovskite remained intact (Fig. 2b). Stiff Surlyn (Table 1), which adheres well to glass and ITO,[29] pulled up on the ITO and delaminated the PSCs, creating a pathway for moisture induced degradation, similar to delamination after thermal cycling test for Surlyn encapsulated PSCs.[10] Therefore it is not suitable for mechanically fragile PSCs. In contrast to EVA and Surlyn, perovskite films in polyolefin packages remained uniformly brown outside and under the top ITO after accelerated testing (Fig. 2c). We think that the polyolefin is less chemically reactive with the perovskite but cannot rule out that it functions better by being less permeable to products that outgas from the perovskite when it decomposes. Not only was the polyolefin observed to have no chemical reaction with perovskite, it also has a low elastic modulus similar to EVA (Table 1), which was demonstrated to withstand the 200 thermal cycle test.[10] Moreover, polyolefin encapsulants have high electrical resistivity, making them less prone to PID, unlike EVA and polyvinyl butyl encapsulant modules.[30] Therefore, we chose polyolefin, which is becoming popular for thin-film panels, for the 2nd generation encapsulant. Since all encapsulants we used are commercially available, we included product numbers in Table 2.

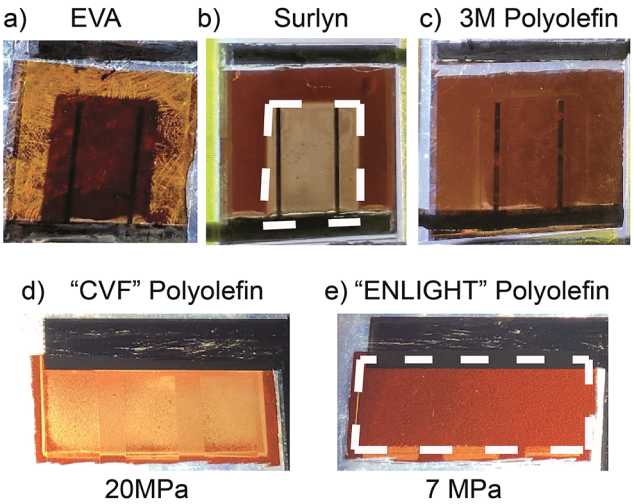

Fig. 2 Pictures taken under a solar lamp of the 1st generation encapsulated PSCs in (a) Ethylene Vinyl Acetate (EVA) (b) Surlyn (c) 3 M's polyolefin after 20 hours at 120 °C-100% relative humidity. Another set of pictures taken under the lamp of the 2nd generation encapsulated PSCs in (d) "CVF" polyolefin with 20 MPa elastic modulus and (e) "ENLIGHT" polyolefin with 7 MPa elastic modulus after 1024 hours aging at 85 °C in ambient. The top protective ITOs are outlined in (b) and (e) as dash rectangles.

In selecting the exact polyolefin, we compared two non-curing polyolefin encapsulants to avoid potential chemical reactions between crosslinking or "curing" residuals and the perovskite. Perovskite films encapsulated in the 2nd generation package with "CVF" (20 MPa elastic modulus) and "ENLIGHT" (7 MPa elastic modulus) were aged at 85 °C in ambient atmosphere. After 1000 hours, we observed discoloration in the packages with a higher elastic modulus (Fig. 2d), which implies

Table 1 Properties of commercial encapsulants used in this study

Properties	Ethylene vinyl acetate	Surlyn	Polyolefin		
Provider	Mitsui Chemicals	Dupont	3 M	DNP "CVF"	FirstPVM "ENLIGHT"
Encapsulation condition	140 °C, 650 mbar 20 min	140 °C, 650 mbar 20 min		150 °C, 500 mbar, 8 min	
Transmittance (%)	93	93.4	91	92	>85
Elastic modulus (MPa)	10	394	9.1	20	7
Possibly harmful byproduct	Acetic acid	Methacrylic acid	Unknown (curing)	Unknown (non-curing)	Unknown (non-curing)

Table 2 Product information of encapsulants used in the study

Encapsulant	Providers	Part number	Thickness per sheet of encapsulant
EVA	Mitsui	RC02B-45T	0.45 mm
Surlyn	Dupont	PV5400	0.2 mm
Polyolefin	3 M	PO8510	0.45 mm
Polyolefin	Dai Nippon Printing	CVF	0.4 mm
Polyolefin	Hangzhou first applied material (FirstPVM)	XUS66250	0.5 mm

degradation of the perovskite that can be explained by the same delamination mechanism as the stiff Surlyn package. On the other hand, PSCs encapsulated in the low elastic modulus polyolefin remained undamaged in the protected area under the ITO (Fig. 2e). As a result, ENLIGHT polyolefin was incorporated into the 2nd generation package of PSCs for further reliability tests. The solar cells chosen in the following reliability studies are ones with PCE above 11% after encapsulation, with some reaching over 14%. All encapsulated PSCs had less than 5% drop in initial performance after lamination (Table S1†). The efficiency in these cells is lower than we report in other studies because of a lower fill factor, due to the large series resistance that results from current traveling a relatively long distance in ITO.

4 Thermal cycling test

Encapsulated PSCs were held for 25 minutes at 85 °C and −40 °C and their stabilized performance was periodically monitored throughout the IEC 61646 200 thermal cycle test. Fig. 3a shows that nine out of nine encapsulated PSCs in three separate packages passed the 200 cycle test, with an average 3% increase in performance. This enhancement in performance came from an average 3% increase in open circuit voltage (V_{OC}) counteracting an average 3% decrease in fill factor (FF), while the short circuit current (J_{SC}) remained relatively constant, Fig. S4.† Fig. 3b and c show no visual sign of perovskite degradation after 200 temperature cycles. Moreover, the package was intact without delamination or blistering (Fig. 3d). With low elastic modulus (Table 1), the ENLIGHT polyolefin dissipated strain due to thermal expansion coefficient mismatch and kept fragile PSCs together during thermal cycling. This result is in agreement with our hypothesis and previous studies[10,19] that a compliant encapsulant material is needed for PSCs to pass the thermal cycling test.

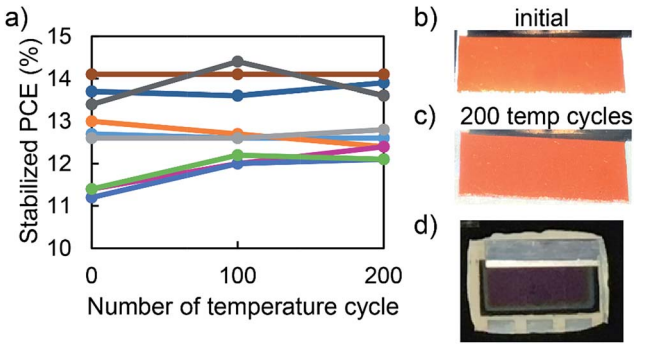

Fig. 3 (a) Stabilized power conversion efficiency of nine solar cells over 200 temperature cycles between −40 °C and 85 °C. Representative picture of the ENLIGHT encapsulated PSCs (b) initial (c) 200 temperature cycles taken under the solar lamp. (d) Top view of a representative package after temperature cycling shows no sign of delamination or blistering.

5 Damp heat and thermal stability test

We investigated heat and moisture stability of the 2nd generation PSC package in a series of experiments. First, we monitored dark storage stability in a nitrogen glovebox at 25 °C and found the packaged PSCs to be stable over 1000 hours with less than five percent change in any figures of merit (Table S2†). To investigate thermal stability without any effect from moisture and oxygen, we compared non-encapsulated and encapsulated PSCs stability at 85 °C in an inert atmosphere over 1000 hours. While some non-encapsulated solar cells retained almost 100% of their performance (Fig. S5†), establishing a good baseline of high thermal stability of our PSCs, reproducibility was a problem with an average 20% drop in performance after 1000 hours. Fig. S6a† further illustrates that without encapsulation, the perovskite area outside the ITO cover degraded to yellow lines of PbI_2, which could explain the drop in fill factor. On the other hand, glass–glass encapsulation helped improve thermal stability at 85 °C in an inert atmosphere and increased reproducibility of the PSCs to retain on average 97% of their initial PCE through the 1000 hour test (Fig. S7†) without visible degradation in the active area (Fig. S6b†). Thus, glass encapsulation is shown to enhance thermal stability of PSCs, likely by providing an additional barrier to organic cation evolution and preventing delamination or cracking of the brittle top ITO electrode layer due to thermal expansion.

To accelerate degradation due to heat and moisture, we aged the encapsulated PSCs for 1000 hours in 85 °C-85% RH damp heat test according to the IEC 61646 standard. We periodically monitored the stabilized performance of the PSCs after maximum power point tracking (details on stabilization in ESI: extracting solar cell performance from “stabilized” state, Fig. S13–S16†). Fig. 4b shows that ten solar cells in five separate packages retained, on average, 99% of their initial PCE (4% V_{OC} increase, 8% FF decrease, and 2% J_{SC} increase), thus passing the damp heat test. Thirteen encapsulated solar cells in five separate packages aged at 85 °C-25% RH (“dry heat”) (Fig. 4a) also

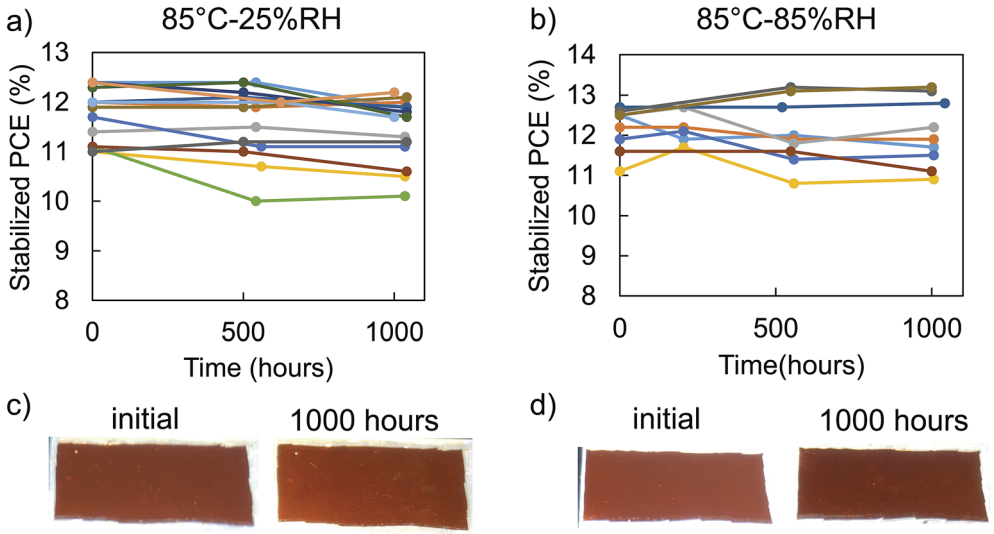

Fig. 4 Stabilized maximum power efficiency for 2nd generation-packaged PSCs with the ENLIGHT polyolefin as they went through (a) 85 °C-25% RH or "dry heat" and (b) 85 °C-85% RH or "damp heat". Representative pictures of the encapsulated solar cells in (c) dry heat (d) damp heat taken under the solar lamp before and after 1000 hours of aging.

retained on average 97% of their PCE (5% V_{OC} increase, 9% FF decrease, and 1% J_{SC} increase). All figures of merit seem to stabilize in the first 500 hours and then change minimally afterwards (Fig. S8 and S9†). With this trend, the encapsulated PSCs should be able to last beyond 1000 hours. We measured photoluminescence quantum efficiency (PLQE) of ITO-encapsulated half solar cell stacks (Fig. S10a†) with either NiO*x* (hole transport layer) or C_{60} (electron transport layer) contacts before and after annealing at 85 °C in an inert atmosphere to investigate potential causes of the seemingly correlated drop in FF and rise in V_{OC}. Fig. S10b and c† show that after 700 hours at 85 °C, the PLQE increased on both half cells, compared with the controls kept at 25 °C. This result indicates a drop in non-radiative recombination rate of the half cells, consistent with the increase in V_{OC}.[31] Moreover, PbI_2 was observed *via* X-ray diffraction in the non-encapsulated solar cells after 1000 hours annealing at 85 °C in inert atmosphere, Fig. S11.† We speculate that even in ITO covered solar cells, small amounts of PbI_2 likely form insulating islands between the perovskite and contact layers, limiting charge extracting pathways.[32–34] This slightly lowers the FF but raises the V_{OC} by limiting charge transfer to the contact at open circuit and raising the quasi Fermi levels within the perovskite layer itself.

Since the performance of dry heat and damp heat were similar, it can be concluded that the 2nd generation package keeps out moisture well and any change in figures of merit came from heat, not moisture. Furthermore, there were no visual changes in the 2nd generation packaged PSCs (Fig. 4c and d) and no change in absorption and external quantum efficiency (Fig. S12†) after 1000 hours in both dry and damp heat tests. Moreover, there were no signs of metal induced degradation, moisture induced degradation, or chemical reaction between the polyolefin and encapsulant. Having passed the 1000 hour damp heat test, the 2nd generation package is capable of protecting the PSCs from heat and moisture induced degradation.

6 Conclusion

Our holistic encapsulation design enabled PSCs to pass the IEC 61646 standard thermal cycling and damp heat tests, showing promise for environmental stability of PSCs with proper packaging and paving the way to future long-term stability testing in the field. We have demonstrated a packaging technique that any research group can use for reliability testing. Moreover, the approach could be scaled and commercialized easily if one simply used standard junction boxes to provide low resistance leak-free paths for electricity to leave the panel.

When forecasting how PSCs might compete with other photovoltaic technologies and whether they should be implemented in ultra-low-cost flexible panels, conventional glass–glass panels, or high efficiency tandems, it is important to create cost models and calculate the levelized cost of electricity (LCOE). This study gives cost modelers a better picture of what materials are likely to be used to package PSCs and how the package will be put together. Moreover, it reveals that a 25 year lifetime is a realistic goal. While we do not report lifetime studies on panels made with less expensive or flexible materials, our experience and calculations based on data available in the literature lead us to believe that a 25 year lifetime would probably not be achieved in very low cost flexible modules unless breakthroughs were made in reducing the permeability of inexpensive plastic substrates. The cost of two sheets of glass, encapsulant and butyl rubber edge seal is approximately $17 per m^2,[35] which is half the of the cost of the module and not prohibitive. In fact the packaging we report is very similar to what First Solar uses for CdTe panels. However, with this moderately high packaging cost, it is important for PSCs to have

an efficiency that is competitive with CdTe and Si to achieve the remarkably low LCOEs that the PSC community is striving for.

7 Experimental methods

7.1. Solar cells fabrication

Both 2 cm × 2 cm × 0.7 mm (1st generation) and 5 cm × 5 cm × 0.7 mm, "big substrate", (2nd generation) indium-doped tin oxide patterned glass substrates from Xin Yan technology were cleaned *via* four sonication steps in Extran, DI water, acetone, and isopropanol, and then put in a UV-ozone cleaner for 15–30 minutes. A 1 M solution of nickel nitrate hexahydrate (Sigma-Aldrich) in ethylenediamine (Sigma-Aldrich) and anhydrous ethylene glycol (Sigma-Aldrich) was spun on the substrates at 5000 rpm for 1 minute. The substrates were then annealed in ambient air at 300 °C for 45 minutes before being transferred to a dry air glovebox while their temperatures were still above 100 °C. The perovskite precursor solution was prepared by mixing CsI (Sigma-Aldrich, 99.99% trace metals), FAI (Dyesol), $PbBr_2$ (TCI), and PbI_2 (TCI) in a mixture of *N*,*N*-dimethylformamide (Sigma-Aldrich) and dimethyl sulfoxide (Sigma-Aldrich) and letting it stir at 25 °C in a nitrogen glovebox for an hour. To reduce the area of perovskite coverage on the 5 cm × 5 cm substrate, PVC Vinyl Nitto tape (SPV224) was used to mask all four sides. The perovskite solution was deposited through a 0.2 μm PTFE filter and spun for 14 seconds at 1000 rpm and then 25 seconds at 6000 rpm. 140 μl chlorobenzene solution was dropped during the last 5 seconds before the substrates finished spinning as an anti-solvent to enhance crystallization, forming $Cs_{0.17}FA_{0.83}Pb(Br_{0.17}I_{0.83})_3$ perovskite composition. The Nitto tape was removed from all sides of the big substrates, and the as-deposited perovskite films were annealed at 52 °C until the color turned dark brown, approximately 1 minute, then at 105 °C for 30 minutes. Afterwards, the substrates were transferred to a dry nitrogen glovebox for thermal evaporation of 1.2 nm LiF and 10 nm of C_{60}. The perovskite on the big substrate was brought out to a fume hood, the film outside the active area was scratched away with a razor blade, wiped with toluene and ethanol, and then blown dry so that there are clean areas for edge seal to bond the top and bottom glass. It is critical to keep the air exposure time during this process below 10 minutes to minimize degradation of perovskite. Then, 8 nm of stoichiometric SnO_2 and 2 nm of zinc doped SnO_2 were deposited consecutively by pulse-chemical vapor deposition at 100 °C. More detailed condition of this deposition step can be found elsewhere.[2] 300 nm of indium-doped tin oxide (ITO) was deposited through D.C. sputtering as the top electrical contact. ITO sputtering was performed with a base pressure below 5×10^{-6} Torr, deposition pressure of 2×10^{-3} Torr, a power density of 8 W in^{-2}, and 5% oxygen partial pressure.[36] As the final step, 250 nm silver was deposited *via* thermal evaporation on the 2 cm × 2 cm substrates, while 7 nm chromium followed by 500 nm silver was deposited on ITO lines on the 5 cm × 5 cm substrates to minimize series resistance. This ITO/metal bilayer design allowed for increased lateral conductivity from the silver with chromium as an adhesion layer for improved scratch resistance of the silver from the underlying ITO.

7.2. Perovskite solar cells encapsulation

To make the 1st generation package, an indium solar ribbon (part number WCD102-7747-6022) was soldered on the evaporated silver electrode on the 2 cm × 2 cm substrate. The butyl rubber edge seal with added desiccant (Quanex, SET LP03: 2.5 mm thick) was laid out as a frame around the outer edge of the glass. The solar cells were assembled between top and bottom sheets of encapsulant and 3 mm thick glass with the solar ribbons sandwiched between two sides of the edge seal (bottom edge seal: 2.5 mm thick, top edge seal: 0.4 mm thick) to minimize moisture ingress. The package was laminated in the vacuum laminator (P. Energy Lab Laminator: L150LAB) in two steps: vacuum was pulled down to 110 Pa while heating the package to 140–150 °C for 5 minutes, then the package was pressed with 6.5×10^4 Pa pressure at 140 °C for 20 minutes for ethylene vinyl acetate and Surlyn ionomer encapsulants, and 150 °C for 8 minutes for polyolefin encapsulants for the edge seal to soften and the encapsulant to cure. The edge seal flattened out during the lamination process, yielding the final width of 10 mm and thickness of 1.5 mm, Fig. 1. Because there was a 0.8 mm thick space surrounding the PSCs (0.7 mm thick) that needed to be filled by encapsulant, the pressing step needed to be gradual with uniform pressure so that the packages were evenly compressed with no built-in stress causing the glass to crack (Fig. S2b†). It is also important to ensure the right amount of encapsulant inside the package to prevent voids or internal stress build-up that can lead to breakage of a package. The thickness variation from the headspace height and the lateral spacing of the encapsulant from the edge seal should be no more than 0.2 mm.

The 2nd generation package was prepared by assembling the edge seal and encapsulant on the top glass, which was made of 1.2 mm thick microscope slides cut to a rectangular size, slightly smaller than the superstrate to allow contact to the electrical feedthrough coming out for performance measurements. The butyl rubber edge seal with added desiccant (Quanex, SET LP03, 0.74 mm) was laid out as a frame on the outer edge of the top glass. The polyolefin sheet was cut to the size of the window framed by outer edge seal. Then the solar cell superstrate was flipped down to finish assembly to the top glass. Afterwards, the assembly was put in the vacuum laminator (Vacuum Laminating Technology: HVFP 24) with the superstrate on the bottom. Vacuum was pulled down to 3×10^3 Pa while letting the assembly heat up from 25 °C to 150 °C for 18 minutes (measured with a thermocouple), then the package was pressed with 6.5×10^4 Pa pressure at 150 °C for 8 minutes. The edge seal flattened out during the lamination process, yielding the final width of 15 mm and thickness of 0.5 mm, Fig. 1.

7.3. Solar cell performance measurement

Current–voltage (*J*–*V*) measurements were performed through a digital source meter, Keithley model 2400, and a LABVIEW control program. Each solar cell was illuminated from the bottom through the hole transport layer, NiO*x*, by a 300 watt xenon lamp (Oriel) solar simulator (Spectra-Physics) through a 0.12 cm^2 aperture mask in air. When adjusting the intensity of

the solar simulator, spectral mismatch was taken into account as in ref. 37 by using an NREL certified KG5 photodiode (Hamamatsu) with known external quantum efficiency (EQE) and spectral response linear with light intensity beyond 1 sun. The photodiode EQE was measured by comparing its response to a NIST traceable reference photodiode. The integrated current from EQE measurement of a solar cell matches well with the short circuit current measured under the solar simulator. (Fig. S17 and Table S3†) the mismatch factor was calculated to be 0.97. The current–voltage was scanned from −0.2 V to 1.3 V with 0.06 V s^{-1} speed and 0.1 s dwell time. Each solar cell was also subjected to maximum power point stabilization and ensured that the power remained constant for 200 seconds. Afterwards, the *J–V* curve was measured in both direction to check for any hysteresis and the figure of merits were extracted from stabilized condition. No hysteresis was found both before and after all different environmental aging (Fig. S18 and S19†).

The external quantum efficiency (EQE) was measured using a Princeton Instruments SpectraPro 150 monochromator and Stanford Research Systems SR830 model lock-ins. The signal from 100 watt tungsten lamp (Newport) was chopped at a frequency around 73 Hz and split with half incident on a reference silicon photodiode and the other half on the solar cell device. The photocurrent response of both devices was recorded as a function of wavelength to account for any fluctuations in lamp intensity. EQE was calculated from comparing the photocurrent of the device to a NIST traceable calibration photodiode.

Absorption spectra of the PSCs were measured in an integrating sphere (LabSphere). The light from a mercury arc lamp was chopped at 136 Hz and coupled into the integrating sphere, hitting the packaged PSCs through the back glass. A silicon photodiode (Newport) was used to measure the absorbed light. The photodiode current was measured through a Stanford Research Systems SR380 lock-in amplifier. The measured photodiode current was normalized by the current from a reference photodiode, split from the path of light before the integrating sphere entry, to account for any change in the power of the lamp.

7.4. Stability testing

7.4.1 Accelerated 120 °C-100% RH test. The accelerated test at 120 °C-100% relative humidity was carried out in a pressure cooker Instant Pot DUO80 (IP-DUO80). The 1st generation packaged solar cells were placed on an elevated rack to avoid submerging in water and the packages were stressed 4 hours at a time. The packages were inspected on the solar simulator lamp for any change in color periodically. Pictures of the initial and aged packaged solar cells placed on top of the solar simulator were taken with a digital camera.

7.4.2 Thermal cycling. The 2nd generation package solar cells in the ENLIGHT polyolefin were loaded in a thermal cycling chamber (Thermotron SE-600-3-3) and stabilized at 25 °C. A full temperature cycle composed of heating the chamber to 85 °C with a rate of 60 °C per minute, holding the chamber at 85 °C for 25 minutes, ramping the temperature down to −40 °C with the same 60 °C per minute rate, and holding the chamber at −40 °C for 25 minutes. The chamber had a set deviation of 4 °C at both 85 °C and −40 °C before the 25 minutes dwell time would start counting. After 100 cycles, the solar cells were taken out of the chamber, allowed to stabilize to room temperature, and measured using maximum power point tracking, before being placed back into the chamber.

7.4.3 Dry heat/damp heat/control in ambient and N_2. Non-encapsulated and 2nd generation package solar cells were aged on an 85 °C hotplate in a nitrogen glovebox with <10 ppm moisture and <10 ppm oxygen for the "inert" condition. The damp (85 °C-85% relative humidity) and dry heat (85 °C-25% relative humidity) experiments were carried out in environmental chambers. The encapsulated solar cells in these two chambers were taken out every 500 hours to measure their performance at room temperature in ambient. At each data point, the solar cells were maximum power point tracked until they reached stabilized performance for at least 200 seconds before the figures of merit were extracted.

7.5. Photoluminescence quantum efficiency measurement

Photoluminescence of half stack solar cells with structure in Fig. S10† was measured at open circuit voltage inside an integrating sphere. The film stack was excited with a 488 nm continuous wave diode laser (Obis) at 100 mW cm^{-2} power and four measurements were carried out according to J. C. de Mello.[38] The four signals were measured using a spectrograph (Acton Research SpectraPro 500i) equipped with a Hamamatsu silicon CCD array detector.

7.6. X-ray diffraction measurement

Samples were measured with an X'Pert Pro Diffractometer (copper anode, $K\alpha_1 = 1.54060$ Å, $K\alpha_2 = 1.54443$ Å, with $K\alpha_1/K\alpha_2 = 0.50$) in air.

Conflicts of interest

There are no conflicts to declare.

Acknowledgements

The information, data and work presented herein were funded in part by the US Department of Energy (DOE) PVRD2 program under award number DE-EE0008154 and the Office of Naval Research under award number N00014-17-1-2525. We thank Wen Ma and Farhad Moghadam at Sunpreme for depositing the ITO electrodes. We thank Duncan Harwood and Shandor Daroczi from D2 solar for their support with encapsulation and reliability testing. We also would like to thank encapsulant companies Mitsui Chemicals, Dupont, 3M, Dai Nippon Printing, and Hangzhou First Applied Material for providing encapsulants along with helpful information. We really appreciated all the support from Quanex, especially Lori Postak for fruitful discussions and materials provision. We also would like to acknowledge insightful discussion with Nick Bosco, Sarah

Kurtz, Michael Kempe, Jared Tracy, Nicholas Rolston, and Reinhold Dauskardt. R. C. acknowledges generous support from the Ministry of Science and Technology of Thailand fellowship. C. B. acknowledges support from the National Science Foundation Graduate Research Fellowship under Grant No. DGE – 1656518. Part of this work was performed at the Stanford Nano Shared Facilities (SNSF), supported by the National Science Foundation under award ECCS-1542152.

References

1 W. S. Yang, B.-W. Park, E. H. Jung, N. J. Jeon, Y. C. Kim, D. U. Lee, S. S. Shin, J. Seo, E. K. Kim, J. H. Noh and S. Il Seok, *Science*, 2017, **356**, 1376–1379.
2 K. A. Bush, A. F. Palmstrom, Z. J. Yu, M. Boccard, R. Cheacharoen, J. P. Mailoa, D. P. McMeekin, R. L. Z. Hoye, C. D. Bailie, T. Leijtens, I. M. Peters, M. C. Minichetti, N. Rolston, R. Prasanna, S. Sofia, D. Harwood, W. Ma, F. Moghadam, H. J. Snaith, T. Buonassisi, Z. C. Holman, S. F. Bent and M. D. McGehee, *Nat. Energy*, 2017, **2**, 17009.
3 T. Leijtens, K. Bush, R. Cheacharoen, R. Beal, A. Bowring and M. D. McGehee, *J. Mater. Chem. A*, 2017, **5**, 11483–11500.
4 B. Conings, J. Drijkoningen, N. Gauquelin, A. Babayigit, J. D'Haen, L. D'Olieslaeger, A. Ethirajan, J. Verbeeck, J. Manca, E. Mosconi, F. De Angelis and H.-G. Boyen, *Adv. Energy Mater.*, 2015, **5**, 1500477.
5 J. Yang, B. D. Siempelkamp, D. Liu and T. L. Kelly, *ACS Nano*, 2015, **9**, 1955–1963.
6 Y. Han, S. Meyer, Y. Dkhissi, K. Weber, J. M. Pringle, U. Bach, L. Spiccia and Y.-B. Cheng, *J. Mater. Chem. A*, 2015, **3**, 8139–8147.
7 M. Saliba, T. Matsui, J.-Y. Seo, K. Domanski, J.-P. Correa-Baena, M. K. Nazeeruddin, S. M. Zakeeruddin, W. Tress, A. Abate, A. Hagfeldt and M. Grätzel, *Energy Environ. Sci.*, 2016, **9**, 1989–1997.
8 J. Zhao, K. O. Brinkmann, T. Hu, N. Pourdavoud, T. Becker, T. Gahlmann, R. Heiderhoff, A. Polywka, P. Görrn, Y. Chen, B. Cheng and T. Riedl, *Adv. Energy Mater.*, 2017, **7**, 1602599.
9 N. Rolston, B. L. Watson, C. D. Bailie, M. D. McGehee, J. P. Bastos, R. Gehlhaar, J.-E. Kim, D. Vak, A. T. Mallajosyula, G. Gupta, A. D. Mohite and R. H. Dauskardt, *Extreme Mech. Lett.*, 2016, **9**, 353–358.
10 R. Cheacharoen, N. Rolston, D. Harwood, K. A. Bush, R. H. Dauskardt and M. D. McGehee, *Energy Environ. Sci.*, 2018, **11**, 144–150.
11 F. Bella, G. Griffini, J.-P. Correa-Baena, G. Saracco, M. Grätzel, A. Hagfeldt, S. Turri and C. Gerbaldi, *Science*, 2016, **354**, 203–206.
12 Y. Il Lee, N. J. Jeon, B. J. Kim, H. Shim, T.-Y. Yang, S. Il Seok, J. Seo and S. G. Im, *Adv. Energy Mater.*, 2018, **8**, 1701928.
13 G. Grancini, C. Roldán-Carmona, I. Zimmermann, E. Mosconi, X. Lee, D. Martineau, S. Narbey, F. Oswald, F. De Angelis, M. Graetzel and M. K. Nazeeruddin, *Nat. Commun.*, 2017, **8**, 15684.
14 F. Matteocci, L. Cinà, E. Lamanna, S. Cacovich, G. Divitini, P. A. Midgley, C. Ducati and A. Di Carlo, *Nano Energy*, 2016, **30**, 162–172.
15 Q. Dong, F. Liu, M. K. Wong, H. W. Tam, A. B. Djurišić, A. Ng, C. Surya, W. K. Chan and A. M. C. Ng, *ChemSusChem*, 2016, **9**, 2518.
16 M. D. Kempe, A. A. Dameron and M. O. Reese, *Prog. Photovoltaics Res. Appl.*, 2014, **22**, 1159–1171.
17 E. F. Cuddihy, B. Baum and P. Willis, *Sol. Energy*, 1979, **22**, 389–396.
18 M. Kempe, in *Photovoltaic Solar Energy*, John Wiley & Sons, Ltd, Chichester, UK, 2017, pp. 478–490.
19 L. Shi, T. L. Young, J. Kim, Y. Sheng, L. Wang, Y. Chen, Z. Feng, M. J. Keevers, X. Hao, P. J. Verlinden, M. A. Green and A. W. Y. Ho-Baillie, *ACS Appl. Mater. Interfaces*, 2017, **9**, 25073–25081.
20 IEC 61646:2008|IEC Webstore|rural electrification, solar power, 2008.
21 D. P. McMeekin, G. Sadoughi, W. Rehman, G. E. Eperon, M. Saliba, M. T. Hörantner, A. Haghighirad, N. Sakai, L. Korte, F. Giustino, *et al.*, *Science*, 2016, **351**, 151–155.
22 Z. Li, M. Yang, J.-S. Park, S.-H. Wei, J. J. Berry and K. Zhu, *Chem. Mater.*, 2016, **28**, 284–292.
23 Y. Kato, L. K. Ono, M. V. Lee, S. Wang, S. R. Raga and Y. Qi, *Adv. Mater. Interfaces*, 2015, **2**, 1500195.
24 K. Domanski, J.-P. Correa-Baena, N. Mine, M. K. Nazeeruddin, A. Abate, M. Saliba, W. Tress, A. Hagfeldt and M. Grätzel, *ACS Nano*, 2016, **10**, 6306–6314.
25 M. D. Kempe, D. Panchagade, M. O. Reese and A. A. Dameron, *Prog. Photovoltaics Res. Appl.*, 2015, **23**, 570–581.
26 M. D. Kempe, D. C. Miller, J. H. Wohlgemuth, S. R. Kurtz, J. M. Moseley, Q. A. Shah, G. Tamizhmani, K. Sakurai, M. Inoue, T. Doi, A. Masuda, S. L. Samuels and C. E. Vanderpan, *Energy Sci. Eng.*, 2015, **3**, 565–580.
27 M. D. Kempe, G. J. Jorgensen, K. M. Terwilliger, T. J. McMahon, C. E. Kennedy and T. T. Borek, *Sol. Energy Mater. Sol. Cells*, 2007, **91**, 315–329.
28 M. Schutze, M. Junghanel, M. B. Koentopp, S. Cwikla, S. Friedrich, J. W. Muller and P. Wawer, in *2011 37th IEEE Photovoltaic Specialists Conference*, IEEE, 2011, pp. 000821–000826.
29 U. Eitner, S. Kajari-Schröder, M. Köntges and H. Altenbach, in *Shell-like Structures. Advanced Structured Materials*, Springer, Berlin, Heidelberg, 2011, pp. 453–468.
30 J. Berghold, S. Koch, B. Frohmann, P. Hacke and P. Grunow, in *2014 IEEE 40th Photovoltaic Specialist Conference (PVSC)*, IEEE, 2014, pp. 1987–1992.
31 O. D. Miller, E. Yablonovitch and S. R. Kurtz, *IEEE J. Photovolt.*, 2012, **2**, 303–311.
32 T. J. Jacobsson, J.-P. Correa-Baena, E. Halvani Anaraki, B. Philippe, S. D. Stranks, M. E. F. Bouduban, W. Tress, K. Schenk, J. Teuscher, J.-E. Moser, H. Rensmo and A. Hagfeldt, *J. Am. Chem. Soc.*, 2016, **138**, 10331–10343.
33 D. H. Cao, C. C. Stoumpos, C. D. Malliakas, M. J. Katz, O. K. Farha, J. T. Hupp and M. G. Kanatzidis, *APL Mater.*, 2014, **2**, 091101.

34 D. Bi, A. M. El-Zohry, A. Hagfeldt and G. Boschloo, *ACS Photonics*, 2015, **2**, 589–594.
35 Z. Song, C. L. McElvany, A. B. Phillips, I. Celik, P. W. Krantz, S. C. Watthage, G. K. Liyanage, D. Apul and M. J. Heben, *Energy Environ. Sci.*, 2017, **10**, 1297–1305.
36 K. A. Bush, C. D. Bailie, Y. Chen, A. R. Bowring, W. Wang, W. Ma, T. Leijtens, F. Moghadam and M. D. McGehee, *Adv. Mater.*, 2016, **28**, 3937–3943.
37 V. Shrotriya, G. Li, Y. Yao, T. Moriarty, K. Emery and Y. Yang, *Adv. Funct. Mater.*, 2006, **16**, 2016–2023.
38 J. C. de Mello, H. F. Wittmann and R. H. Friend, *Adv. Mater.*, 1997, **9**, 230–232.